Saudi Pharmaceutical Journal 26 (2018) 1120–1126

Contents lists available at ScienceDirect

Saudi Pharmaceutical Journal

journal homepage: www.sciencedirect.com

Radioiodination and biodistribution of newly synthesized 3-benzyl-2-([3-methoxybenzyl]thio)benzo[*g*]quinazolin-4-(3*H*)-one in tumor bearing mice

Rashad Al-Salahi [a,*], Moustapha E. Moustapha [b], Hatem A. Abuelizz [a], Abdulrahman I. Alharthi [b], Khalid A. Alburikan [c], Ismail T. Ibrahim [d], Mohamed Marzouk [b,e], Mohamed A. Motaleb [d]

[a] *Department of Pharmaceutical Chemistry, College of Pharmacy, King Saud University, P.O. Box 2457, Riyadh 11451, Saudi Arabia*
[b] *Department of Chemistry, College of Science and Humanities, Prince Sattam bin Abdulaziz University, P.O. Box 83, Al Kharj 11942, Saudi Arabia*
[c] *Department of Clinical Pharmacy, College of Pharmacy, King Saud University, P.O. Box 2457, Riyadh 11451, Saudi Arabia*
[d] *Labeled Compound Department, Hot Laboratories Centre, Atomic Energy Authority, P.O. Box 13759, Cairo, Egypt*
[e] *Chemistry of Natural Products Group, Center of Excellence for Advanced Sciences, National Research Centre, Dokki, Cairo 12622, Egypt*

A R T I C L E I N F O

Article history:
Received 29 March 2018
Accepted 5 June 2018
Available online 06 June 2018

Keywords:
Benzo[*g*]quinazoline
Radioiodination
Biodistribution
Tumor cell
NBS

A B S T R A C T

3-Benzyl-2-((3-methoxybenzyl)thio)benzo[*g*]quinazolin-4(3*H*)-one was previously synthesized and proved by physicochemical analyses (HRMS, ^{1}H and ^{13}C NMR). The target compound was examined for its radioactivity and the results showed that benzo[*g*]quinazoline was successfully labeled with radioactive iodine using NBS via an electrophilic substitution reaction. The reaction parameters that affected the labeling yield such as concentration, pH and time were studied to optimize the labeling conditions. The radiochemical yield was 91.2 ± 1.22% and the *in vitro* studies showed that the target compound was stable for up to 24 h. The thyroid was among the other organs in which the uptake of ^{125}I-benzoquinazoline has increased significantly over the time up to 4.1%. The tumor uptake was 6.95%. Radiochemical and metabolic stability of the benzoquinazoline *in vivo*/*in vitro* and biodistribution studies provide some insights about the requirements for developing more potent radiopharmaceutical for targeting the tumor cells.

1. Introduction

Thyroid cancer is considered the most common cancer among the endocrine malignancy. Its prevalence is highly increasing in over the last few decades (Pellegriti et al., 2013). The current treatment involves thyroidectomy. Radioactive iodine is administered post operation to oblate any remaining tissue. However, the radioactive therapy relies on the iodine absorption by the thyroid gland and concentrates the exposure to the tumor site (Cooper et al., 2009). Although some small molecule represented promising antitumor agents, sorafenib has been shown by clinical studies it is beneficial in thyroid cancer. Sorafenib is a small molecule that has been approved to be used in advanced thyroid carcinoma and specifically for radioactive iodine resistant (Espinosa et al., 2017). Thus, further studies are needed to identify new compounds for this purpose (Fig. 1).

Benzoquinazolines, as the theme of much considerable interest research, have occupied a distinguished position in synthetic-pharmaceutical chemistry, because of their diverse range of pharmacological properties (Al-Salahi et al., 2016; 2017; Brullo et al., 2012). Several benzo[*h*]-,benzo[*g*]-and benzo[*f*] analogues of quinazolines were found to possess cytotoxic activities and used as tyrosine kinase inhibitors (Huijun, 2017; Nowak et al., 2014; Nowak et al., 2015; Markosyan et al., 2010; Pendergast et al., 1994; Alsaid et al., 2017; Sivalingam et al., 2017; Ghorab et al., 2016; Al-Salahi et al., 2015). For instance, 3-(4-methoxybenzyl)-6-(morpholin -4-yl)benzo[*h*]quinazolin-4(3*H*)-one was reported to exhibit high cytotoxic effect against human colorectal adenocarcinoma cell lined HT29 with IC_{50} value of 4.12 μM in relation to cisplatin (IC_{50} = 8.47 μM) (Nowak et al., 2014). This successful achieved results became an evident support to the further research

* Corresponding author.
E-mail address: ralsalahi@ksu.edu.sa (R. Al-Salahi).
Peer review under responsibility of King Saud University.

ELSEVIER Production and hosting by Elsevier

https://doi.org/10.1016/j.jsps.2018.06.001
1319-0164/

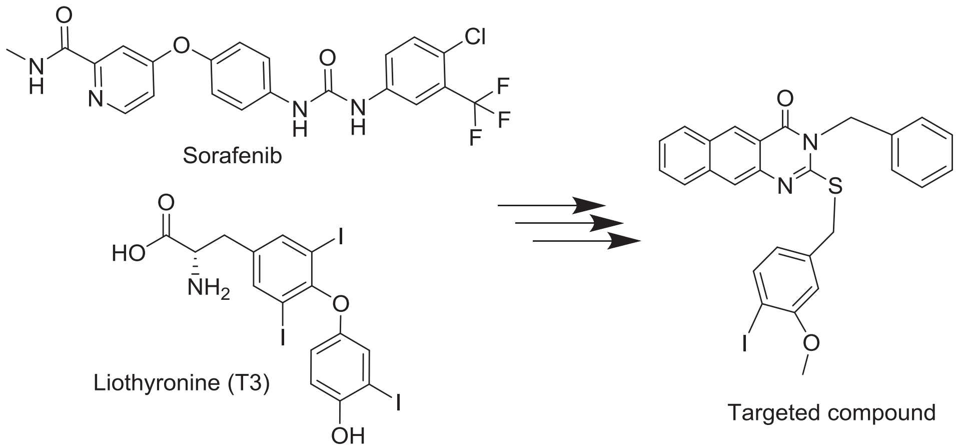

Fig. 1. Representative examples of reported anticancer (Sorafenib) T3 hormone and the designed benzoquinazoline.

on the benzo[*h*]quinazoline scaffold, thus amino-benzo[*h*]quinazoline derivatives were developed and their obtained findings demonstrated high specific cytotoxicity against HT29 and HCT116 cell lines (Nowak et al., 2015). At the same time, bromo benzo[*h*]quinazoline was emerged to exhibit potential cytotoxicity against A549 and HT29 cell lines (Nowak et al., 2015). Condensation some benzo[*h*]quinazolines into spiro-compounds with cyclic hydrocarbons exhibited antineoplastic property (Markosyan et al., 2010) Furthermore, screening some derivatives bearing benzo[*f*] quinazoline skeleton for their anticancer effects was found as potent thymidylate synthase inhibitors (Pendergast et al., 1994). An array of some new benzo[g]quinazolines bearing benzenesulfonamide moiety showed high activity against A549 lung cancer cell line (IC_{50} = 0.12–8.70 μM) and exhibited the highest activity towards EGFR and HER2 with IC_{50} values of 0.06 and 0.30 μM, respectively in relation to erlotinib (IC_{50} = 0.73 μM) (Alsaid et al., 2017). A number of dimethoxy(dimethylamino) phenyl)-3,4-dihydrobenzo[g]quinazoline-2,5,10-trione derivatives were active against A549 cell and showed high affinity towards anaplastic lymphoma kinase receptor (Sivalingam et al., 2017). Moreover, some novel series of benzo[*g*]quinazolines bearing the sulfonamide and sulfonyl groups were described as potent antitumor agents (Ghorab et al., 2016). As a part of our interest in the search for more active cytotoxic benzoquinazolines, 2-thioxo-benzo[*g*]quinazoline series were synthesized and evaluated against different carcinoma cell lines including prostate PC-3, lung A-549, colon HCT-116, hepatocellular Hep-G2, and breast MCF-7. Many of the synthesized 2-thioxo-benzo[g]quinazolines have shown significant cytotoxic effects in relation to doxorubicin (Al-Salahi et al., 2015). Chemical modifications study on our 2-thioxo-benzo[g]quinazolines supplied us with some valuable information about the required properties needed benzo[*g*]quinazolines to be more potent anticancer agents.

Anticancer radiopharmaceuticals are generally designed to deliver selectively radionuclides that emit charged particles, such as α particles (^{213}Bi, ^{211}At, ^{225}Ac, ^{227}Th and ^{223}Ra), β (^{131}I, ^{90}Y and ^{177}Lu) or Auger electrons (^{125}I, ^{123}I and ^{111}In), to cancer cells via a targeting molecules (Jackson et al., 2013; Barbet et al., 2012; Carlsson, 2012; Cornelissen and Vallis, 2010; Leyton et al., 2011; Brady et al., 2013; De Jong et al., 2005; Baidoo et al., 2013). A large number of anticancer agents have been labeled with radioactive iodine for targeting cancer cells (Haberkorn et al., 2017; Svetlana et al., 2016; Divgi and Thou, 2014; Van Nostrand, 2009; Mier et al., 2014; Kreissl et al., 2010). Electrophilic labeling via oxidative radioiodination technique was used with N-Bromosuccinimide (NBS) or chloramine-T (CAT) as a source of active oxidizing species for the formation of positively charged iodine (I^+). Iodonium ion is generated *in situ* as the electrophile for radioiodination of the benzoquinazoline. This type of radioiodination reaction usually proceeds in high radiochemical yield (Moustapha et al., 2013; Motaleb et al., 2011). Thus, the current study aims to synthesize a new 2-thioxo-benzo[g]quinazoline derivative bearing benzyl group at position 3 (R = benzyl; R_1 = 3-methoxybenzyl; Fig. 2), incorporating radioiodine and biological evaluation in tumor cells.

2. Materials and methods

2.1. Chemicals

No-carrier-added potassium iodide (NCA $K^{125}I$, 3.7 GBq/ml in 0.1 N NaOH) was purchased from Institute of Isotopes, Budapest, Hungary. N-Bromosuccinimide [$C_4H_4BrNO_2$ (NBS)], sodium thiosulfate ($Na_2S_2O_3$) and methanol were purchased from Sigma-Aldrich.

2.2. No-carrier-added radioiodination of benzoquinazoline

In presence of NBS, direct electrophilic substitution with NCA $K^{125}I$ ($t_{1/2}$ = 60 days) was employed to synthesize ^{125}I-benzoquinazoline. High specific activity iodide (^{125}I) affords the advantage to use high radioactivity radioisotope without adding carrier iodine. Several reaction parameters as NBS concentration, benzoquinazoline concentration (100–1000 μg), pH (1–9) and the reaction time (1–90 min) were investigated and optimized in order to maximize the radiochemical yield and enhanced radioiodination efficiency. A two-neck (25 mL) round bottomed flask was used for radioiodination (fitted with a reflux condenser on one neck; the other neck was fitted with rubber stopper for withdrawing samples and immersed in a thermostatically controlled water bath). NCA $K^{125}I$ (3.7 MBq) was transferred to the reaction vessel. A freshly amount NBS (1000 μg) was prepared in methanol and added to the reaction flask, then benzoquinazoline (500 μg) in methanol was added. The pH of the reaction mixture was adjusted to 4 using a buffer solution. The mixture was left to stir at RT for 30

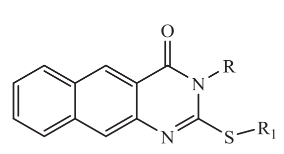

1: R= *n*-butyl, R_1= benzyl
2: R= *n*-butyl, R_1= 3-methoxybenzyl
R= benzyl, R_1= 3-methoxybenzyl (target)

Fig. 2. The structures of the analogues (1, 2) and the target.

min. A drop of saturated sodium thiosulfate (10%) was added to the reaction mixture to decompose the excess of iodine (I_2) in order to stop its reducing into iodide (I^-) as it is oxidized to tetrathionate ($S_4O_6^{2-}$). The radiolabeled benzoquinazoline was gathered and its radiochemical yield was determined by TLC (Moustapha et al., 2013; Motaleb et al., 2011).

2.3. Analysis of ^{125}I-benzoquinazoline

A drop of the reaction mixture (1–2 µl) was placed 2 cm above the edge of TLC strip (1 cm width, 13 cm length) and allowed to evaporate spontaneously. Using a freshly prepared mixture of CH_2Cl_2: EtOAc (2:1 v/v) to develop the strips in order to determine radiochemical yield and purity of ^{125}I-benzoquinazoline. The radiochemical yield was further confirmed by reversed phase-HPLC (RP-HPLC). The compound was purified by HPLC for *in vivo* biodistribution studies. An aliquot of 25 µl of ^{125}I-benzoquinazoline at the optimum conditions was injected into a RP C18 column (Agilent, 250 × 4.6 mm; 5 µm) kept at room temperature using a mobile phase consisting of 0.1 M sodium phosphate buffer and acetonitrile (60:40, v/v) adjusted to pH 2.5 at a flow rate of 1.00 mL/min. The radiolabeling yield and selectivity/specificity of the radioiodinated compound were evaluated after formulation and purification by the same procedure.

2.4. Stability of ^{125}I-benzoquinazoline in serum

An aliquot of normal serum (1 mL) was mixed with ^{125}I-benzoquinazoline (0.5 mL) and incubated for 24 h at 37 °C. During the incubation, aliquots (0.2 mL) were withdrawn at different time intervals up to 24 h and subjected to TLC to estimate ^{125}I-benzoquinazoline percentage and free iodine. Thus, the stability of the radiolabeled complex will determine its suitability for *in vivo* application (Motaleb et al., 2011).

2.5. Induction of solid tumor in mice

Ehrlich ascites carcinoma was the parent tumor line. The cell lines driven from a seven days old donor mouse were diluted with sterile saline. Approximately 0.2 mL of the solution was injected intramuscularly in the right thigh to produce a solid tumor for 4–6 days.

2.6. Biodistribution studies of ^{125}I-benzoquinazoline

Biodistribution studies were carried out in accordance with the guidelines adopted by the Egyptian atomic energy authority and authorized by the animal ethics committee, labeled compound department. Biodistribution studies of ^{125}I-benzoquinazoline in solid tumor bearing mice (n = 5), were performed at 5, 15, 30, 60 and 180 min post injection (pi). Animals were housed in groups of five and provided with water and food. Aliquots of 5 µl containing 4 mbq of the purified radiolabeled complex were injected into each mice via the tail vein. Each mouse was isolated before sacrifice by cervical dislocation at 5, 15, 30, 60 and 180 min after administration of ^{125}I-benzoquinazoline (n = 5). The weight of each animal was estimated and the blood was drawn from the heart and weighed directly after sacrifice. The animals were dissected, the organs and tissues were rinsed with saline, samples of fresh blood, bones (femoral bone) and muscles (left thigh muscle) were collected in plastic containers and weighed. The background and the radioactivity of each sample were counted in a well-type nai (tl) well crystal coupled to sr-7 scaler ratemeter. Percent injected dose per organ (% id/organ ± s.d.) in a population of five mice for each time point are reported (Motaleb et al., 2011).

3. Results and discussion

3.1. Chemistry

As reported by Al-Salahi et collaborators, treatment the intermediate (**A**) with 3-methoxybenzyl bromide in boiling DMF in the presence of triethylamine (Scheme 1) afforded smoothly 3-benzyl-2-((3-methoxybenzyl)thio)-benzo[*g*]quinazolin-4(3*H*)-one (**B**) (Al-Salahi et al., 2018). The target **B** was characterized by the convenient physicochemical methods and finally established by NMR and HRMS analyses (Al-Salahi et al., 2018).

3.2. *Radiolabeling of the target benzo[g]quinazoline (B)*

The radiochemical yield of ^{125}I-benzoquinazoline was estimated by TLC using a developing eluent system of CH_2Cl_2: EtOAc (2:1 v/v). Radioiodide (^{125}I) remained near the origin (R_f = 0–0.1), while the iodo compound (^{125}I-benzoquinazoline) moved with the eluent front (R_f = 0.8–1). The ratio of the radioactivity of ^{125}I-benzoquinazoline to the total radioactivity multiplied by 100 was recorded for determination the radiochemical yield percentage. The labeling yield was 91.4 ± 1.62% (n = 3). It was further confirmed by HPLC analysis, where the retention time of free iodide and ^{125}I- atorvastatin were 1.9 and 5.3 min, respectively, as presented in the chromatogram (Fig. 3). The HPLC system allowed the separation of the labeled compound from the free iodide, the unlabeled benzoquinazoline as well as the purification and quality control assessment of the compound. The theoretical specific activity of the NCA ^{125}I-benzoquinazoline injected was 2.75×10^7 Ci/mol. The yield of ^{125}I-benzoquinazoline is the mean value of three experiments. The factors affecting the yield percentage of ^{125}I-benzoquinazoline will be explained in details. As illustrated in Scheme 2, the iodobenzoquinazoline (**C**) was obtained from reaction of benzoquinazoline (B) with $K^{125}I$ in the presence of NBS as oxidizing agent and radiochemical yield was determined by TLC (see experimental part). There are many reaction parameters that affected the labeling yield such as concentration, pH, time and oxidizing agent (Moustapha et al., 2013).

Fig. 4 depicted the effect of benzoquinazoline amount on radiochemical yield. The reaction carried out at different concentration of benzoquinazoline (10–100 µg). Increasing the yield from 82.5 to 91.2% was associated with increasing benzoquinazoline concentration from 50 to 200 µg. However, the increasing in benzoquinazoline concentration above 200 µg had no effect on the labeling yield. This indicates that benzoquinazoline (above 200 µg) might be capable to react with the entire generated iodonium ion (I^+). Accordingly, the labeling yield attained maximum value (91.2 ± 1.22%) at this concentration (50–200 µg). By increasing the amount of NBS from 50 to 500 µg as shown in Fig. 5, a high radiochemical yield (91.2 ± 1.22%) was afforded. The low percentage of ^{125}I-bnezoquinazoline (80.7%) correlated with NBS might be due to the bromination of the active benzene ring of benzoquinazoline that compete with the iodination procedure. Increasing the NBS concentration above 500 µg leads to a stability in the iodination yield. This is caused due to the formation of unacceptable oxidative by-products like bromination, denaturation and polymerization of benzoquinazoline. These impurities might be referred to the concentration and high reactivity of NBS. Therefore, the optimal concentration of NBS was necessary to prevent the formation of by-products and to obtain the maximum purity and yield.

The radiochemical yield depends greatly on the reaction time ranged between 1 and 90 min. Fig. 6 shows that the yield was elevated when increasing the reaction time from 1 to 60 min. However, increasing the reaction time above 60 min leads to a slight reduction in the labeling yield (85.5%). The maximum radiochem-

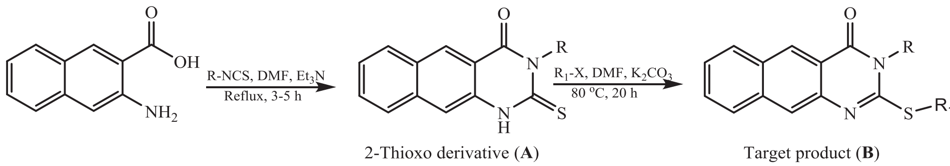

Scheme 1. Synthesis of the target compound, where R = benzyl and R1 = 3-methoxybenzyl.

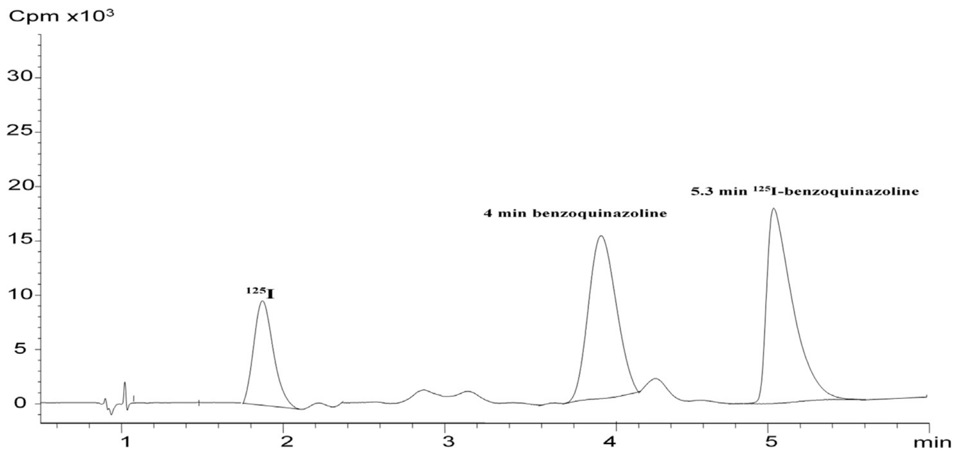

Fig. 3. Overlaid chromatograms of benzoquinazoline and ^{125}I-benzoquinazoline.

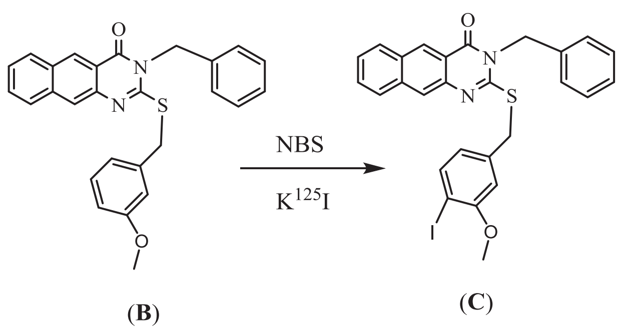

Scheme 2. synthetic route for Iodobenzoquinazoline (**C**).

ical yield (91.2 ± 1.22%) was obtained when the mixture was allowed to react for 60 min. At a reaction time above 60 min, the labeling yield is decreased due to the exposure of the substrate to highly reactive NBS for longer time, which leads to oxidative side reactions. On the other hand, when NBS was allowed to react with iodide for short time, the iodonium ion was generated minimally, in which consequently the obtained yield was low (~66%) below 60 min.

The radiochemical yield of ^{125}I-bnezoquinazoline was affected by the pH as shown in Fig. 7. At the pH ranged between 1 and 9, the reaction medium was investigated. NBS is known as mild selective oxidizing agent. It has been used for bromination and dehydrogenation of organic compounds. NBS is a source of iodonium ion (I^+) that can act in both acidic and alkaline solutions. The pos-

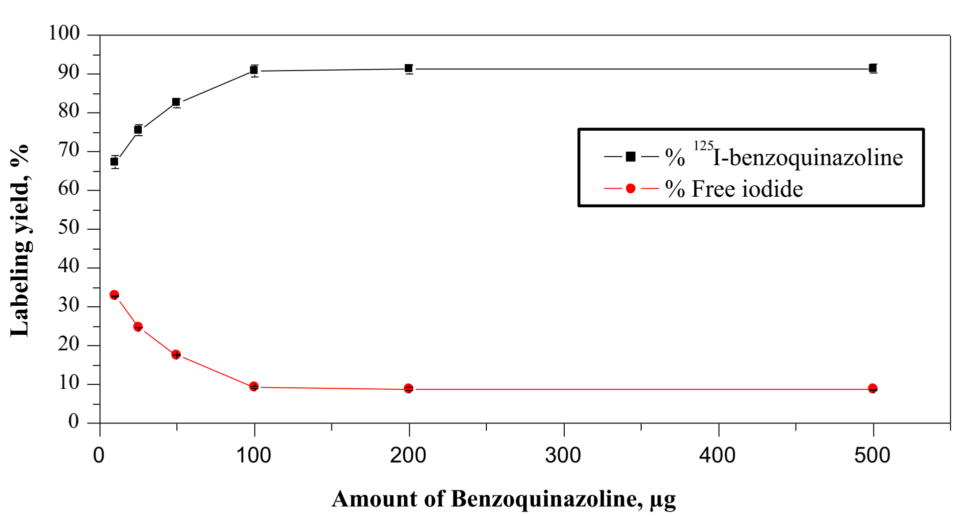

Fig. 4. Variation of the labeling yield of ^{125}I-benzoquinazoline as a function of different amounts of benzoquinazoline ; conditions: xµg benzoquinazoline, 500 µg of NBS, 0.5 mL (3.7 MBq) of NCA^{125}I- at pH 4, the reaction mixture was kept at room temperature for 60 min.

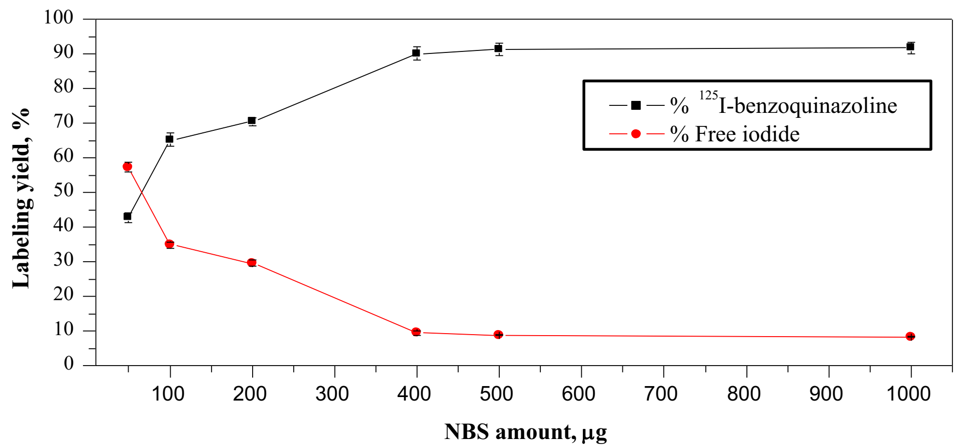

Fig. 5. Variation of the labeling yield of ^{125}I-benzoquinazoline as a function of of NBS concentration; ;reaction conditions: 100 µg benzoquinazoline, x µg of NBS, 0.5 mL (3.7 MBq) of NCA^{125}I- at pH 4, the reaction mixture was kept at room temperature for 60 min.

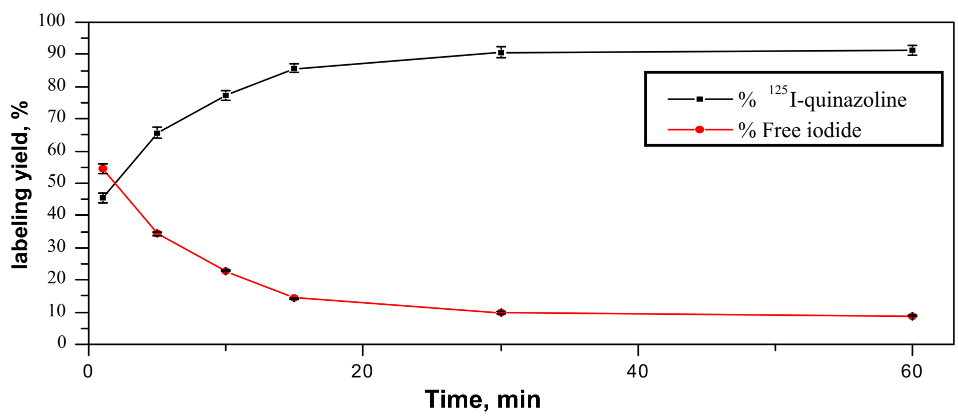

Fig. 6. Variation of the labeling yield of ^{125}I-benzoquinazoline as a function of reaction time; reaction conditions: 100 µg benzoquinazoline, 500 µg of NBS, 0.5 mL (3.7 MBq) of NCA^{125}I- at pH 4, the reaction mixture was kept at room temperature for x min.

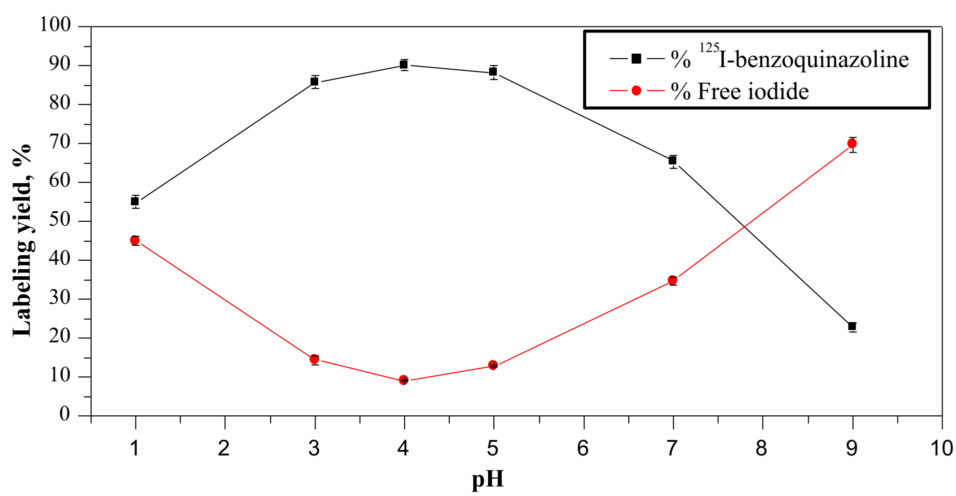

Fig. 7. Variation of the labeling yield of ^{125}I-benzoquinazoline as a function of pH; reaction conditions: 100 µg benzoquinazoline, 500 µg of NBS, 0.5 mL (3.7 MBq) of NCA^{125}I- at pH = x, the reaction mixture was kept at room temperature for 60 min.

sible reactive species of NBS in acidic solution are NBS itself or Br^+ or protonated NBS viz., RN^+HBr. At pH 4, the yield was maximized (90.2%) due to the protonation of the aromatic ring at this pH is giving H^+, which was substituted by the iodonium ion. As the pH was deviated towards the acidic side, the labeling yield decreased to 65.3% and 55% at pH 6.5 and pH 1, respectively. While the yield

Table 1
In vivo biodistribution analysis (% ID/g ± S.D., n = 5) of ^{125}I-benzoquinazoline in normal Sprague-Dawley mice at different time intervals post injection.

Organs and body fluids	% injected dose/g at different time intervals (min)				
	5	15	30	60	180
Blood	18.92 ± 0.12	17.25 ± 0.25	14.43 ± 0.13	11.36 ± 0.42	5.40 ± 0.31
Bone	0.31 ± 0.03	0.55 ± 0.10	0.8 ± 0.05	1.25 ± 0.12	1.3 ± 0.314
Muscle	0.9 ± 0.01	1.5 ± 0.25	1.9 ± 0.16	2.4 ± 0.18	2.7 ± 0.07
Liver	12.3 ± 0.15	15.7 ± 0.32	16.9 ± 0.28	14.2 ± 0.41	7.8 ± 0.22
Spleen	0.2 ± 0.00	0.25 ± 0.10	0.3 ± 0.06	0.33 ± 0.12	0.4 ± 0.05
Lung	2.56 ± 0.21	2.9 3 ± 0.42	2.75 ± 0.19	2.42 ± 0.25	2.16 ± 0.01
Stomach	1.35 ± 0.34	2.51 ± 0.19	6.55 ± 0.15	7.36 ± 0.43	5.41 ± 0.35
Heart	4.42 ± 0.23	3.71 ± 0.30	2.90 ± 0.16	2.23 ± 0.04	1.34 ± 0.09
Intestines	2.15 ± 0.01	2.54 ± 0.12	3.62 ± 0.25	5.45 ± 0.35	4.33 ± 0.21
Kidneys	1.26 ± 0.14	4.47 ± 0.10	4.93 ± 0.19	6.85 ± 0.48	6.35 ± 0.39
Thyroid	0.57 ± 0.38	0.95 ± 0.42	1.79 ± 0.31	2.35 ± 0.28	4.10 ± 0.19
Tumor muscle	1.47 ± 0.89	2.49 ± 0.58	3.28 ± 0.78	5.49 ± 0.38	6.95 ± 0.93
T leg	1.51 ± 0.23	2.75 ± 0.41	3.76 ± 0.51	3.94 ± 0.78	3.72 ± 0.60
N leg	1.24 ± 0.52	1.36 ± 0.36	1.89 ± 0.18	1.15 ± 0.08	1.12 ± 0.21

was very poor reaching 22.7% at pH equals to 9. The radiochemical yield was decreased at alkaline pH due to the complete dissociation of NBS.

3.3. Stability of ^{125}I-benzo[g]quinazoline

In vitro stability of the labeled compound was performed to determine the suitable time for injection to prevent the composition of the unacceptable products that accompany the radiolysis of ^{125}I-benzoquinazoline. These undesired radioactive by-products may be concentrated in non-target organs. The obtained results indicated that ^{125}I-benzoquinazoline was stable up to 24 h.

3.4. Biodistribution of ^{125}I-benzo[g]quinazoline in tumor bearing mice

Table 1 showed the biodistribution of ^{125}I-benzoquinazoline in different organs and in the tumor. The results are expressed as average percent injected dose per gram of the tissue or organ (% ID/g). The data showed substantial uptake of 4.42% ID/g in the cardiac muscle at 5 min post injection (pi), while the radioactivity declined to 3.71 at 15 min pi. From 30 min pi until 180 min pi, radioactivity levels decreased to 1.34. After 30 min the uptakes of radiolabeled benzoquinazoline are showed in liver (16.9), kidney (4.93), intestines (3.62), stomach (6.55), lungs (2.75) and thyroid (1.79). The uptake of ^{125}I-benzoquinazoline is decreased over the time except for thyroid and stomach, which demonstrated increased significantly over the time. The small dose located in the thyroid gland indicated that ^{125}I-benzoquinazoline was stable *in vivo* against biological decomposition. The tumor uptake (6.95%) was showing that ^{125}I-benzoquinazoline was able to target the cells with reasonable radioactivity suitable for radiotherapy. This finding can be used as a targeted treatment to the thyroid. The distribution of the percentage of the injected compound at the thyroid can be reduced to reach the optimum radiotherapeutic dose that is suitable for the organ size and reduces the effect on the other organs.

4. Conclusions

Applying direct electrophilic substitution and using NBS, benzoquinazoline was radioiodinated with NCA ^{125}I in a high labeling yield (91.2%). Characterization of ^{125}I-benzoquinazoline *in vitro* and *in vivo* was described in this study. Biodistribution studies manifested the ^{125}I-benzoquinazoline affinity towards tumor cells with 6.95% injected dose per organ. Moreover, the ^{125}I-benzoquinazoline has demonstrated a significant increase in the uptake by the thyroid gland compared to the other organs. This is essential for developing more potent radiopharmaceutical for targeting the tumor cells.

Acknowledgements

The authors extend their appreciation to the Deanship of Scientific Research at King Saud University for funding this work through research group No. RG-1439-011.

Conflict of interest

The authors declare no conflict of interest and are responsible for the content and writing this article.

References

Alsaid, M., Al-Mishari, A.A., Soliman, A.M., Ragab, F.A., Ghorab, M.M., 2017. Discovery of Benzo[g]quinazolin benzenesulfonamide derivatives as dual EGFR/HER2 inhibitors. Eur. J. Med. Chem. 141, 84–91.

Al-Salahi, R., Abuelizz, H.A., El-Dib, R., Marzouk, M., 2017. Antimicrobial activity of new 2-Thioxo-benzo [*g*]quinazolin-4(3*H*)-one derivatives. Med. Chem. 13, 85–92.

Al-Salahi, R., Abuelizz, H.A., Ghabbour, H.A., El-Dib, R., Marzouk, M., 2016. Molecular docking study and antiviral evaluation of 2-thioxo-benzo[*g*]quinazolin-4(3*H*)-one derivatives. Chem. Cent. J. 19 (10), 21.

Al-Salahi, R., Ahmad, R., Anouar, E., Nor Izzati, I.N.A., Marzouk, M., Abuelizz, H.A., 2018. 3-Benzyl(phenethyl)-2-thioxobenzo[*g*]quinazolines as a new class of potent α-glucosidase inhibitors: synthesis and molecular docking study. Future Med. Chem. https://doi.org/10.4155/fmc-2018-0141.

Al-Salahi, R., El Dib, R.A., Marzouk, M., 2015. Synthesis and in vitro cytotoxicity evaluation of new 2-thioxo-benzo[g]quinazolin-4(3H)-one derivatives. Heterocycles 91, 1735–1751.

Baidoo, K.E., Yong, K., Brechbiel, M.W., 2013. Molecular pathways: targeted alpha-particle radiation therapy. Clin. Cancer Res. 19, 530–537.

Barbet, J., Bardies, M., Bourgeois, M., et al., 2012. Radiolabeled antibodies for cancer imaging and therapy. Methods Mol. Biol. 907, 681–697.

Brady, D., Parker, C.C., O'Sullivan, J.M., 2013. Bone-targeting radiopharmaceuticals including radium-223. Cancer J. 19, 71–78.

Brullo, C., Rocca, M., Fossa, P., Cichero, E., Barocelli, E., et al., 2012. Synthesis of new 5,6-dihydrobenzo[*h*]quinazoline 2,4-diamino substituted and antiplatelet/antiphlogistic activities evaluation. Bioorg. Med. Chem. Lett. 22, 1125–1129.

Carlsson, J., 2012. Potential for clinical radionuclide-based imaging and therapy of common cancers expressing EGFR-family receptors. Tumour Biol. 33, 653–659.

Cooper, D.S., Doherty, G.M., Haugen, B.R., Kloos, R.T., et al., 2009. Revised American Thyroid Association management guidelines for patients with thyroid nodules and differentiated thyroid cancer. American Thyroid Association (ATA) Guidelines Taskforce on Thyroid Nodules and Differentiated Thyroid Cancer. Thyroid 19, 1167–1214.

Cornelissen, B., Vallis, K.A., 2010. Targeting the nucleus: an overview of Auger-electron radionuclide therapy. Curr. Drug Discov. Technol. 7, 263–279.

De Jong, M., Breeman, W.A.P., Valkema, R., et al., 2005. Combination radionuclide therapy using 177Lu and 90Y-labeled Somatostatin analogs. J. Nucl. Med. 46, 13S–17S.

Espinosa, A.V., Porchia, L., Ringel, M.D., 2017. Targeting BRAF in thyroid cancer. Br. J. Cancer. 96, 16–20.

Divgi, C., Thou, W.G., 2014. Radiopharmaceutical therapy. J. Nucl. Med. 55, 5–6.

Ghorab, M.M., Alsaid, M.S., Al-Dosary, M.S., El-Gazzar, M.G., 2016. In-vitro anticancer evaluation and docking study of novel benzo[g]quinazoline-sulfonamide derivatives. Med. Chem. 12, 448–456.
Haberkorn, U., Mier, W., Kopka, K., et al., 2017. Identification of Ligands and Translation to Clinical Applications. J. Nucl. Med. 58, 27S–33S.
Huijun, G., 2017. Diethoxy benzoquinazoline tyrosine kinase inhibitors, its preparation method and application. Faming Zhuanli Shenqing, CN106749369 A 20170531.
Jackson, M.R., Falzone, N., Vallis, K.A., 2013. advances in Anticancer Radiopharmaceuticals. Clin. Oncol. 25, 604–609.
Kreissl, M., Hahner, S., Fassnacht, M., Haenscheid, et al., 2010. 131I-Iodometomidate - A new radionuclide therapy for advanced adrenocortical cancer. J. Nucl. Med. 51, 337.
Leyton, J.V., Hu, M., Gao, C., et al., 2011. Auger electron radioimmunotherapeutic agent specific for the CD123+/CD131– phenotype of the leukemia stem cell population. J. Nucl. Med. 52, 1465–1473.
Markosyan, A.I., Gabrielyan, S.A., Arsenyan, F.G., Sukasyan, R.S., 2010. Synthesis, antineoplastic and antimonoamineoxidase activity of 3-allyl-4-oxo-2-thioxo-1,2,3,4,5,6-hexahydrospiro (benzo[*h*] quinazoline -5,1'–cyclohexanes). Pharm. Chem. J. 44, 405–408.
Mier, M., Kratochwil, C., Hassel, J.C., et al., 2014. Radiopharmaceutical therapy of patients with metastasized melanoma with the melanin-binding benzamide 131I-BA52. J. Nucl. Med. 55, 9–14.
Motaleb, M.A., Moustapha, M.E., Ibrahim, I.T., 2011. Synthesis and biological evaluation of 125I-nebivolol as a potential cardioselective agent for imaging β1-adrenoceptors. J. Radioanal. Nucl. Chem. 289, 239–245.
Moustapha, M.E., Motaleb, M.A., Ibrahim, I.T., Moustafa, M.E., 2013. Oxidative radioiodination of aripiprazole by chloramine-T as a route to a potential brain imaging agent: a mechanistic approach. Radiochemistry 55, 116–122.
Nowak, M., Malinowski, Z., Fornal, E., Zwiak, A.J.O., et al., 2015. Substituted benzoquinazolinones. Part 2: Synthesis of amino-, and sulfanyl-derivatives of benzo[*f*]- and benzo[*h*]quinazolinones. Tetrahedron 71, 9463–9473.
Nowak, M., Malinowski, Z., Zwiak, A.J., et al., 2014. Substituted benzoquinazolinones. Part 1: Synthesis of 6-aminobenzo[*h*]quinazolinones via BuchwaldeHartwig amination from 6-bromobenzo[h]quin zolinones. Tetrahedron 70, 5153–5160.
Pellegriti, G., Frasca, F., Regalbuto, C., Squatrito, S., Vigneri, R., 2013. Worldwide increasing incidence of thyroid cancer: update on epidemiology and risk factors. J. Cancer Epidemiol.. 965212.
Pendergast, W., Dickerson, S.H., Dev, I.K., et al., 1994. Benzo[*f*]quinazoline inhibitors of thymidylate synthase: methyleneamino-linked aroylglutamate derivatives. J. Med. Chem. 37, 838–844.
Sivalingam, L., Dharman, G., Narayanan, R., Arul, A.S., 2017. Synthesis, molecular docking, DFT calculations and cytotoxicity activity of benzo[*g*]quinazoline derivatives in choline chloride-urea. J. Mol. Struct. 1150, 88–95.
Svetlana, N., Waser, R.B., Pozzo, L.D., Tönnesmann,, et al., 2016. Approaches to improve the pharmacokinetics of radiolabeled glucagon-like peptide-1 receptor ligands using antagonistic tracers. J. Nucl. Med. 57, 1282–1288.
Van Nostrand, D., 2009. The benefits and risks of I-131 therapy in patients with well-differentiated thyroid cancer. Thyroid 19, 1381–1391.